

# Jet Preferred Mode vs Shear Layer Mode

M. Mair,<sup>1</sup> M. Bacic,<sup>1</sup> K. Chakravarthy,<sup>1</sup> and B. Williams<sup>1</sup>

Department of Engineering Science, University of Oxford, Oxford OX2 0EQ, United Kingdom

The effect of acoustic excitation on a low Reynolds number jet with constant centreline velocity  $u_0$  but varying velocity profile  $u(y)$  is investigated experimentally using Particle Imaging Velocimetry (PIV). Different initial conditions at the nozzle orifice are here used with the intent to characterise the relation between the jet preferred mode  $f_p$  and the natural shear layer mode  $f_n$ . The jet response to acoustic excitation is described in terms of the centreline velocity decay and the downstream increase in momentum thickness. This study intends to shed some light onto the duality of the two most fundamental flow instabilities and their controversial dependency on each other.

## I. INTRODUCTION

The effect of perturbation of free shear layers has been the subject of numerous fundamental flow control studies since the discovery of coherent vortical structures in turbulent flows. This is because the development and characteristics of free shear layers are of immense importance for practical applications as well as for the understanding of fundamental fluid dynamics. Free shear layers not only lay down the rules of entrainment and noise generation but also dictate the requirements of flow control actuators used to control, for instance, flow separation or turbulence suppression. Since the early 60s researchers around the world have used acoustic excitation to alter the characteristics of free shear layers and to visualise orderly structure in jet turbulence<sup>1</sup>. From a fundamental point of view this has not only shown that turbulence is in fact less random as initially thought but also that entrainment and hence mixing is determined by instabilities found in both the jet centreline and the shear layer. Two different modes, expressed as Strouhal numbers  $St$ , have since then been the focus of a huge amount of published articles, namely the shear layer mode at  $St_\theta = \frac{f_\theta}{u_0} = 0.012$  and the jet preferred mode at  $St_D = \frac{f_D}{u_0} = 0.3$ . The shear layer mode relates the jet centreline velocity  $u_0$  and momentum thickness to the frequency of shedding vortices whereas the jet preferred mode is based on the nozzle height  $h$  or diameter  $D$  (for axisymmetric jets) and is often referred to the passage frequency at the end of the potential core<sup>2</sup>. What's more is that the jet preferred mode, also called the jet column mode, is often shown to exhibit the strongest jet response if artificially excited at that particular frequency<sup>3</sup>. In addition, it has been shown in numerous experimental studies that the jet preferred mode varies from 0.2 to 0.6<sup>2</sup>. This was often attributed to disturbances in the environment of individual facilities<sup>4</sup>. Based on linear stability analysis, the current interpretation of the shear layer and jet preferred mode is that the former develops into the later by successive pairing events meaning that the preferred mode is actually a shear layer mode and both can be considered a global instability<sup>2,5</sup>. This assumption is often undisputed despite any confirmative proof. Only a handful of researchers state that it is indeed more complex; Birbaud et al<sup>6</sup> and Gutmark & Ho<sup>4</sup>, for example, write that "*the question is not completely settled*" and "*the relation [...] has not been fully resolved yet*", respectively. Samimy et al<sup>3</sup> further state that "*it is not clear from the literature how to get from the most amplified mode to the jet preferred mode*". Apart from that, it also

needs to be pointed out that linear stability analysis cannot be used unconditionally for a high Reynolds number jet since using its mean flow as base flow for stability analysis is still a controversial issue in the stability field. Hence, when reviewing the literature, one needs to carefully distinguish the results between laminar and turbulent flows as well as between experimental and analytical methods. Furthermore, given that the preferred mode might as well depend on non-linear phenomena, and hence cannot be captured by linear stability analysis, all subsequent referenced studies regarding the value of the jet preferred mode are experimental studies only. There is, however, other methods which capture well the most energetic modes in a jet. Such methods, although not part of this study, are, for instance, Proper Orthogonal Decomposition<sup>7,8</sup> (POD) as well as resolvent analysis<sup>9–11</sup>. The latter being a powerful tool which can be used to identify frequency dependent modes that are optimal in terms of their linear gain.

Based on recent studies in our laboratory there is evidence suggesting that the jet preferred mode is in fact independent of the shear layer mode. Hence, this paper intends to shed some light onto this matter. The approach taken is to identify the jet preferred mode based on the jet response to acoustic excitation at different initial conditions but constant  $Re$ . By doing so we intend to change the frequency of the shear layer instability while keeping all parameters that quantify the preferred mode Strouhal number ( $\frac{f_p D}{u_0}$ ) constant. A shift of the preferred mode Strouhal number to higher frequencies as the momentum thickness increases would then provide evidence that the jet preferred mode depends on the shear layer mode.

The paper is structured as follows; Part II serves as an additional review that highlights some of the major contributions to the understanding of shear layer instabilities published since the 1970s. It also lays down the grounds of the hypotheses made in this paper. Part III discusses the experimental set-up as well as the prevalent flow and excitation parameters. Experimental results are then presented in Part IV. This is further done for both forced and unforced shear layers. Finally, Part V concludes this study.

## II. BACKGROUND AND HYPOTHESES

The name 'jet preferred mode' originates from Crow & Champagne and refers to an excitation frequency that leads to the highest fluctuating amplitude before saturation<sup>1</sup>. Using Reynolds numbers between  $10^2 - 10^5$  they further found that

the preferred mode scales with the nozzle diameter  $D$  so that  $St_D = 0.3$ . The two dominant characteristics of the jet preferred mode were identified in numerous studies up to super sonic conditions<sup>12</sup> and  $Re = 10^6$  and can be summarized as:

- Roll-up of large coherent structures and the absence of any downstream pairing event<sup>1,3,13–15</sup>
- Maximum increase in entrainment causing the end of the jet potential core to move upstream<sup>1,3,13–15</sup>

The shear layer mode, sometimes called the most unstable mode or Kelvin-Helmholtz instability, refers to the frequency at which the shear layer rolls up into vortical structures. The shear layer mode scales with the initial momentum thickness  $\theta$  so that  $St_\theta = \frac{f_n \theta}{u_0} = 0.012$ <sup>16</sup>. The dominant characteristics of the shear layer mode can be summarized as:

- The power spectrum of a natural free shear layer contains a most amplified frequency  $f_n$  causing the initial roll-up of vortical structures<sup>2,17–19</sup>
- The location of the shear layer roll-up coincides with the non-linear saturation of  $f_n$ <sup>2,20–22</sup>
- Subharmonic components of  $f_n$  which are generated during the growth of  $f_n$  provoke the downstream pairing of neighbouring vortices before the end of the potential core<sup>2,16,23</sup>

The pioneering work of Crow & Champagne in the early 1970ies triggered an avalanche of studies that investigated the spatio-temporal evolution of vortical structures in circular and non-circular as well as forced and unforced jets. In the vast majority of these studies the jet preferred mode is considered to be the passage frequency of vortices at the end of the potential core. For the present authors, however, it is not clear how this became the common point of view. Indeed, the frequency of the jet preferred mode, first determined by Crow & Champagne<sup>1</sup> to be at  $St_D = 0.3$ , is below the shear layer mode and therefore might approach one of its subharmonics at the end of the potential core. It is, however, still inconclusive to equate those two frequencies. This is also because the passage frequency of vortices at the end of the potential core in the experiments of Crow & Champagne amounts to  $St_D = 0.44$ <sup>1,24</sup>, a rarely cited finding. Moreover, the initial definition of the preferred mode required artificial forcing of the jet. This makes it somewhat arbitrary that many studies identified the jet preferred mode by, for example, placing a hotwire inside an unforced jet. The huge scatter regarding the value of the jet preferred mode Strouhal number might therefore as well be a huge scatter of the subharmonic shear layer mode being based on the wrong length-scale. A convincing argument supporting that statement is seen in Fig.1. Experimental studies that have identified the jet preferred mode by the jet response to some sort of artificial forcing correspond to references A (see Tab.1). The value of the preferred mode Strouhal number ranges from 0.28 to 0.35. The Reynolds numbers used vary between  $10^2 - 10^6$ . Studies that have identified the jet preferred mode without any means of forcing correspond to

references B (see Tab.1). The value of the preferred mode Strouhal number ranges here from 0.24 to 0.64. The graph contains all references from Gutmark & Ho<sup>4</sup> who try to explain the variation of the reported preferred mode Strouhal numbers by spatially coherent disturbances in individual facilities. The graph also contains additional studies of the last two decades to reinforce the present hypothesis. Note that the studies from Kibens<sup>25</sup> and Bechert & Pfizenmaier<sup>26</sup> presented in the study of Gutmark & Ho<sup>4</sup> are not considered since they only measure the radiated noise spectrum. Spectral peaks in the acoustic field do not necessarily indicate the jet preferred mode since pairing of neighbouring vortices was shown to be the main source of sound production in a jet and there is no subharmonic component for the excitation of the jet preferred mode<sup>25,27,28</sup>.

TABLE I: Identified jet preferred mode Strouhal numbers of different studies. References A correspond to experimental studies that used some means of forcing the jet. References B correspond to studies that identify the jet preferred mode without artificial forcing

Study	$Re$	$St_D$
<b>References A:</b>		
Crow & Champagne <sup>1</sup>	$10^2 - 10^5$	0.3
Chan <sup>29</sup>	$10^4$	0.35
Samimy et al <sup>3</sup>	$10^6$	0.33
Kim et al <sup>30</sup>	$10^5$	0.3
Samimy et al <sup>12</sup>	$10^6$	0.3
Hussain & Zaman <sup>31</sup>	$10^4 - 10^5$	0.3
Speth & Gaitonde <sup>32</sup>	$10^6$	0.3
<b>References B:</b>		
O'Neill et al <sup>33</sup>	$10^3$	0.78
Ko & Davies <sup>34</sup>	$10^5$	0.43
Fuchs <sup>35</sup>	$10^5$	0.46
Petersen <sup>36</sup>	$10^4$	0.24
Drubka <sup>37</sup>	$10^4$	0.42
Kim & Choi <sup>38</sup>	$10^4$	0.4 – 0.55
Bi et al <sup>39</sup>	$10^4$	0.25
Raman et al <sup>40</sup>	$10^5$	0.4 – 0.5
Browand & Laufer <sup>41</sup>	$10^3$	0.31 – 0.64
Megerian & Karagozian <sup>42</sup>	$10^3$	0.4
Yule <sup>43</sup>	$10^3$	0.5
Getsinger et al <sup>44</sup>	$10^3$	0.49
Landers & Disimile <sup>45</sup>	$10^3$	0.35

Moreover, it is more plausible that natural disturbances in individual facilities affect the shear layer mode and hence its subharmonics rather than the jet preferred mode. This ought to say that random disturbances as well as turbulence intensity - or rather the interaction of both - might as well feature a spectral peak at  $f^*$  which is in the vicinity of the shear layer mode. If the amplitude of  $f^*$  is similar to the initial instability under 'clean' conditions it is reasonable to assume that the shear layer mode locks on to  $f^*$  despite no change in the initial conditions. Note that the turbulent intensity is often around 1 – 3% and therefore in the same order of magnitude as the forcing level.

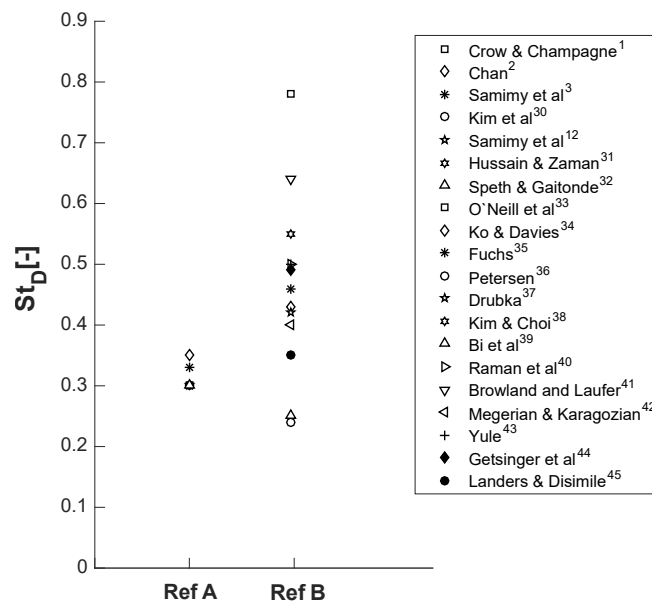


FIG. 1: Reported values for the jet preferred mode. References A correspond to studies that use artificial forcing. References B correspond to studies that determine the jet preferred mode by means of the unforced jet characteristics

One can also argue that, in case the jet preferred mode was the subharmonic at the end of the potential core, the excitation at that frequency should provoke pairing rather than discourage it completely. The open literature, however, does not provide any explanation why the excitation of the jet preferred mode causes large coherent vortical structures that do not undergo pairing. Furthermore, the so-called lock-on effect, which leads to a frequency of the jet response that is equal to the forcing frequency, also produces stable vortices that do not undergo pairing<sup>2</sup>. And given that the required excitation amplitude to achieve the lock-on effect increases significantly as the excitation frequency moves away from the most-amplified frequency, it seems plausible that the preferred mode might just be a lock-on effect at a frequency that is furthest away from both the natural mode and its subharmonic and therefore requiring the highest forcing amplitude which again causes the highest entrainment. The fact that the jet preferred mode requires higher forcing amplitudes is also confirmed by Samimy et al<sup>3</sup> and Crow & Champagne<sup>1</sup>. Based on the arguments made above the three hypotheses made in this paper can be summarized as follows:

- 1.) The jet preferred mode is not a local shear layer instability and hence not related or dependent on the most unstable mode of a jet
- 2.) The jet preferred mode can only be identified by some kind of artificial forcing
- 3.) The huge scatter of the jet preferred mode Strouhal number reported in the literature is in fact the variation of a subharmonic of the shear layer roll-up frequency due to differences in initial conditions

On the basis of those hypotheses, an experiment was set up so to investigate the response of an acoustically excited free circular jet with respect to different initial conditions. Different initial conditions, i.e. different nozzle exit velocity profiles at constant  $Re$ , affect the shear layer roll-up frequency and hence the frequency of paired vortices<sup>46</sup>. The effect of different velocity profiles on the shear layer development was also investigated by Xu & Antonia<sup>47</sup>, though, without forcing. They showed that a larger initial shear layer thickness produces a dimensionally lower frequency instability that results in vortical structures that develop and pair further downstream. Regarding the hypotheses made above, such a shift of the initial instability frequency should not have an effect on the Strouhal number preference that yields the highest response to acoustic excitation. However, irrespective of all plausible arguments supporting that hypothesis one might also argue that the power spectrum at the end of the potential core still shows the same spectral peaks despite different initial roll-up frequencies. A constant preferred mode Strouhal number would therefore not necessarily indicate that the jet preferred mode is independent of the shear layer mode. This again is further complicated by the fact that the end of the potential core shifts upstream as the initial momentum thickness decreases. Thus the question arises at which downstream location the spectral peaks should be compared to each other. Nonetheless, it will be shown later that the results of this study do not support this argument. Besides all that, there is also no lack in controversy in the open literature regarding the effect of initial conditions themselves. While Xu & Antonia<sup>47</sup> found no effect of initial conditions on the self similar region of a jet ( $x > 30D$ ) but clear differences in the near field, Hussain & Zedan<sup>48,49</sup> as well as George<sup>50</sup> found substantial differences in all regions of the jet.

### III. EXPERIMENTAL SET-UP AND PARAMETERS

The light sheet from a dual-head Nd:YAG laser that produces a beam at  $532nm$  with  $600mJ$  per pulse is used to reproduce the velocity vector field in the near-field of the jet (see Fig.2). The laser is passed through cylindrical and spherical lenses to form it into a thin sheet with a thickness of approximately  $0.5mm$ . The flow is seeded with Di-Ethyl-Hexyl-Sebacate (DEHS) using a LaVision aerosol generator. The droplet size ranges between  $0.3$  and  $1\mu m$ . The particle density is controlled by two mass flow controllers (Omega FMA2609A & FMA5520A) and a bypass route. Image pairs are acquired using a high-speed charge-coupled device (CCD) camera (Bobcat B1621) with a fixed inter-frame time of  $200ns$ . A calibration grid is used to set the focus, correct for optical distortion and scale the vector units to  $\frac{m}{s}$ . Dark images of a laser illuminated test section are further obtained and subtracted from all acquired images so to remove background light and impurities of the perspex sheet. The laser inter-pulse time is set so that an average particle displacement of approximately 8 pixels per frame is achieved. A standard decreasing window size multipass processing is further used to calculate the velocity vector field. The ini-

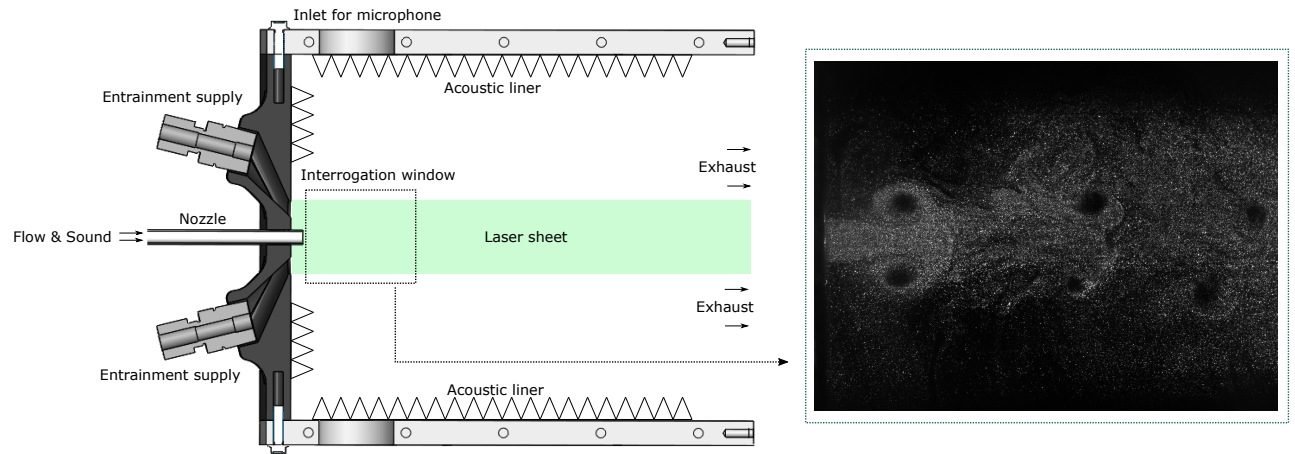


FIG. 2: Top view schematic of the experimental set-up (left) and example snapshot of an excited jet (right)

tial, second and third pass uses a 128x128, 64x64 and 32x32 pixel interrogation window, respectively. A 50% overlap is used for all passes to improve spatial resolution. Processed images use a vector-validation filter that removes individual vectors that exceed a predetermined range and reinserts them based on an interpolation scheme. The Stokes number based on the average particle size and the average nozzle exit velocity never exceeds 0.1. Errors associated with tracing accuracy are therefore around 1%. The mass flow controllers have an accumulated uncertainty of 2.5%.

The test section is a perspex box with a 3D printed cover plate, as shown in Fig.3. The cover plate consists of an opening with  $D = 7.5\text{ mm}$  and an additional circumferential slot through which low speed seeded air ( $< 0.5 \frac{m}{s}$ ) is introduced. Tubes with various lengths are further inserted through the opening centred in the middle. Sound is introduced in an upstream 3D printed box in which seeded and non-seeded air are mixed. The sound source is a 50 Watt Visaton round cabinet speaker (FRS 8 4 OHM) connected to a Tektronix signal generator (AFG1022) and a 40W power amplifier (Kemo Electronic M034N). Acoustic liner is used in both the upstream mixing box as well as the perspex box so to keep resonances and acoustic reflections to a minimum. An omnidirectional condenser microphone (Kingstate MKD-7690) is inserted through a side opening (see Fig.3) and measures the sound pressure level at  $x = 1D$  downstream of the nozzle orifice. A schematic side view together with an example image is shown in Fig 2.

The laser is fired at either 10 Hz or 7.6 Hz. The former is used so to take advantage of aliasing noting that the excitation frequency is always a multiple of 10 Hz. The latter is chosen arbitrarily.

Given the finite width of the laser sheet of approximately 30 mm, the nozzle diameter is set to 7.5 mm. This still allows to capture a full flow field with jet spreading angles that lead to a jet width of more than  $3D$  within the region of interest. The centreline velocity  $u_0$  was chosen so that a root-mean-square sinusoidal surging of up to 2% of the exit speed could

be achieved<sup>1</sup>. This is further based on the maximum amplitude  $\hat{p}$  that can be achieved for all frequencies within the bandwidth of the acoustic speaker. With  $\hat{p} = 133\text{ dB}$  and the acoustic impedance  $\rho c$  this leads to

$$u_0 = \frac{u'}{0.02 \cdot \sqrt{2}} = \frac{\hat{p}}{\rho c \cdot 0.02 \cdot \sqrt{2}} \approx 8 \frac{m}{s} \quad (1)$$

This in turn leads to a hypothetical preferred excitation frequency of 320 Hz ( $St_D = 0.3$ ) and a Reynolds number of 4000. To cover a sufficient range of frequencies below and above the jet preferred mode the excitation frequency  $f_{ex}$  will be varied from 80 to 640 Hz in steps of 20 Hz.

Different initial conditions at the nozzle orifice are then obtained by changing the nozzle length. The four nozzle lengths  $l_N$  considered in this study are 7, 11, 38 and 80  $D$ . The velocity profile for the smallest nozzle is nearly irrotational and features a relatively small momentum thickness  $\theta$ . The longest nozzle, in contrast, has a more fully developed velocity profile with a larger momentum thickness at the orifice. This will be shown later. The jet velocity is kept constant for all  $l_N$  and the non dimensional excitation frequency is varied from  $St_D = 0.1$  to 0.6. The preferred mode Strouhal number is then identified by means of the jet response as a function of  $St_D$ . The upstream shift of the end of the potential core as well as the widening of the shear layer serve here as a quantitative measure of the jet response. The microphone further ensures a constant sound pressure level of 133 dB.

#### IV. FLOW VISUALISATION STUDIES

##### A. Unforced Jet Dynamics

The jet dynamics of the baseline cases, i.e. no excitation, are presented first. Fig.4 a.) and b.) show the centreline velocity decay at constant flow rate  $\dot{m}$  and constant exit velocity

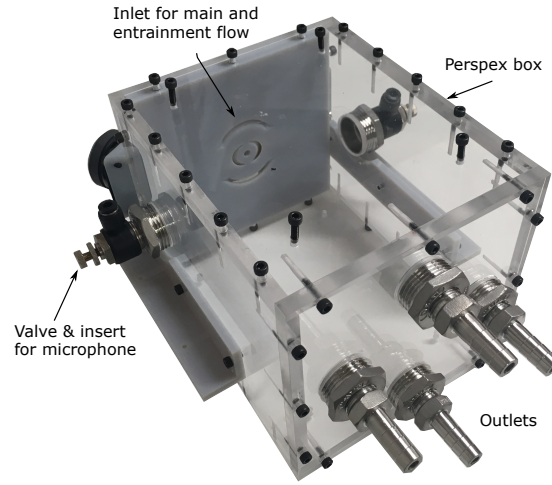
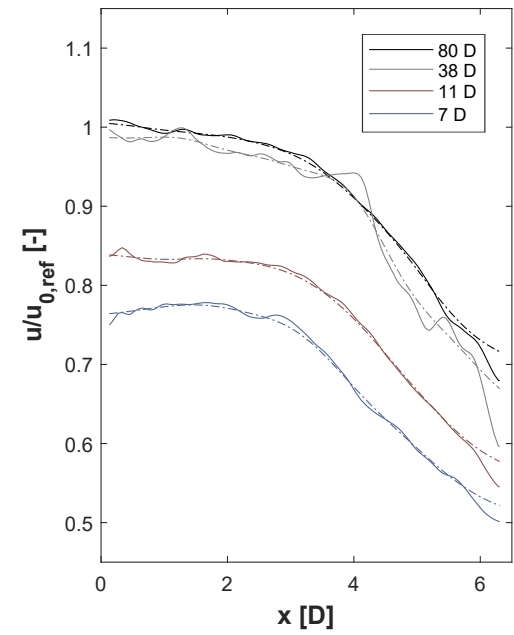


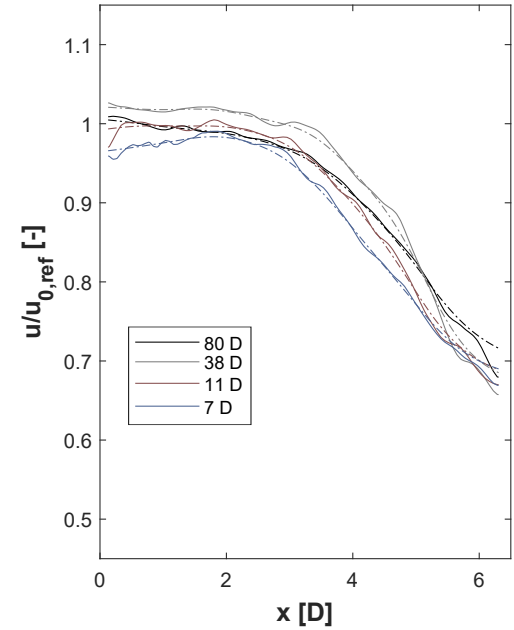
FIG. 3: Test section of the circular jet excitation PIV experiments

$u_0$ , respectively. At constant  $\dot{m}$  it becomes apparent that the different nozzle lengths represent different stages during the development of a velocity profile towards its fully developed state. The centreline velocity for the shortest nozzle (7D) is 25% below the centreline velocity of the longest nozzle (80D). Given the conservation of mass this indicates a more uniform (top-hat) velocity profile for the nozzle with  $l_N = 7D$ . The velocity profile of the longest nozzle, in contrast, is fully developed (boundary layers have merged) since there is essentially no difference between the exit velocity  $u_0$  for  $l_N = 38D$  and  $80D$ . In order to maintain the same Reynolds number based on the centreline velocity at the nozzle orifice  $Re = \frac{u_0 D}{\nu}$  the flow rate  $\dot{m}$  has to increase as the nozzle length  $l_N$  decreases. As can be seen in Fig.4 b.) the flow rate  $\dot{m} = f(l_N)$  is set so to keep the centreline velocity within 3% of  $u_{0,ref} = 8 \frac{m}{s}$ . The end of the potential core  $x_{pc}$  varies between  $\approx 3D$  and  $\approx 3.5D$  in both figures a.) and b.) (when based on  $u_{x_{pc}} = 0.95u_0$  as done in<sup>51</sup>). This is in perfect agreement with the results from Grandchamp & Hirtum<sup>51</sup> who investigated two different nozzle lengths  $l_N = 1.2D$  and  $53.2D$  and obtained a normalized potential core extent of  $\frac{x_{pc}}{D} = 2.9$  and  $3.3$  for the same Reynolds number  $Re = 4000$ , respectively. Note that the dashed lines in Fig.4 represent the smoothed centreline velocity decay which will be used for all future calculations regarding the length of the potential core.

The effect of the different nozzle lengths on the downstream development of the jet becomes even more apparent if the velocity profiles normal to the flow direction are considered. This can be seen in Fig.5 which shows the radial velocity distribution for different axial positions  $\frac{x}{D}$  and different nozzle lengths  $l_N$ . There is no noticeable difference between the relative decay of the jet centreline velocity for both nozzle lengths upstream of  $\frac{x}{D} = 2.5$ . However, it is evident that the centreline velocity of the shorter nozzle ( $l_N = 7D$ ) decays faster downstream of that. This is shown by a slight difference at  $y = 0$  and  $x > 2.5D$ . However, even more obvious are the different



(a)



(b)

FIG. 4: Velocity decay of the jet centerline for different nozzle lengths. X axis expressed in nozzle diameters D. a.) Velocity decay at constant mass flow rate  $\dot{m}$ , b.) Velocity decay at constant nozzle exit velocity  $u_{0,ref}$

shapes of the velocity profile especially at  $\frac{x}{D} = 1$ . The shorter nozzle exhibits a more uniform velocity distribution around  $y = 0$  resulting in greater shear. This again leads to higher vorticity and hence an earlier roll-up of the shear layer. In addition, the frequency of the shear layer roll-up also increases with respect to a longer nozzle since the momentum thickness at the nozzle orifice is smaller. An earlier roll-up as well as

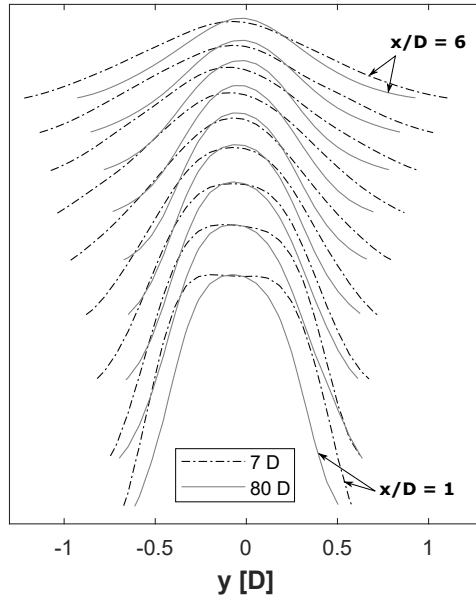


FIG. 5: Non-dimensional radial velocity profile at different downstream locations  $x/D = [1, 2, 3, 4, 5, 6]$

a higher frequency ultimately leads to more entrainment and hence to a wider shear layer and a faster decay of  $u_0$ . The spreading of the shear layer for all four nozzle lengths as a function of  $x$  is shown in Fig.6. It can be seen that a shorter nozzle length causes a larger shear layer for  $\frac{x}{D} > 3.5$  indicating that  $\frac{d\theta}{dx}$  increases as the nozzle length decreases. This is again a measure for the entrainment rate as well as the spreading angle. One can conclude that a shorter nozzle increases the shear layer roll-up frequency, shifts the roll-up location further upstream and causes a faster decay of  $u_0$  which is synonymous to a wider shear layer, higher  $\frac{d\theta}{dx}$  or enhanced entrainment. This is again in perfect agreement with previous results obtained by, for instance, Russ & Strykowski<sup>46</sup>, Xu & Antonia<sup>47</sup> or Kim & Choi<sup>38</sup> who showed that an increase in the initial boundary layer thickness leads to an increase in the streamwise location where vortices start to roll up and undergo pairing as well as a decrease in the instability frequency.

It was also mentioned previously that the possibility exists that the frequency at the end of the potential core remains the same despite a change of the initial conditions. This assumption is indeed not completely unjustified since a lower momentum thickness at the nozzle orifice (shorter nozzle) is shown to cause a higher  $\frac{d\theta}{dx}$  which in turn leads to the fact that at some downstream location  $x_x$  the momentum thickness of each shorter nozzle will coincide with momentum thickness of the longest nozzle. Now, if the ratio  $\frac{u_{0,x_i}}{\theta_{x_i}}$  at  $x_x$  is constant and  $x_x$  further corresponds to the end of the potential core - assuming that the non-dimensional vortex passage frequency based on the local momentum thickness  $\theta$  is constant along  $x$  - the frequency at the end of the potential core would be the same for each nozzle length and different initial conditions. A constant jet preferred mode Strouhal number ( $St_D = 0.3$ ) would therefore not indicate whether the pre-

ferred mode is independent of the shear layer mode or not. However, the results obtained from the present experiments do not show such a behaviour. This is shown in Fig.7. The initial roll-up frequency is shown to be higher for all shorter nozzle lengths with respect to  $l_N = 80D$ . The bigger gradient of  $\frac{d\theta}{dx}$  for shorter nozzles causes the ratio  $\frac{u_{0,x_i}}{\theta_{x_i}}$  and hence the vortex passage frequency to decrease faster. The location  $\frac{x_x}{D}$  at which the passage frequency of  $l_N = 7, 11$  and  $38D$  matches the frequency of  $l_N = 80D$  varies from 2 to 3.7 and therefore doesn't coincide with the respective ends of the potential cores ( $\frac{x_{pc}}{D} = 3 - 3.5$ ). The difference in  $\frac{u_{0,x_i}}{\theta_{x_i}}$  at  $x_{pc}$  between  $l_N = 7D$  and  $l_N = 80D$  is not huge and one might hesitate to draw a definite conclusion. However, Antonia & Zhao<sup>52</sup> also conclude that there is a difference in the vortex passage frequency at  $x_{pc}$  for different initial conditions, albeit not huge. Most striking for the present authors is that the frequency of passing vortices at the end of the potential core decreases as the nozzle lengths decreases. This can only mean that the more uniform velocity profiles with greater shear lead to more pairing events. Here, Fig.7 reveals that there are no pairing events for  $l_N = 80D$  but at least one pairing event for, for example,  $l_N = 11D$ . This is seen by the halving of  $\frac{u_{0,x_i}}{\theta_{x_i}}$  from  $x_0$  to  $x_{pc}$ .

Having examined the effect of initial conditions on the natural jet dynamics the following highlights the dynamics under the combined effects of different initial conditions and acoustic excitation.

## B. Excitation at Constant Reynolds Number

The effect of excitation on the flow field of the jet is exemplarily shown in Fig.8. The first two velocity vector fields correspond to the baseline case, i.e. no excitation, and  $St_D = 0.3$ , respectively. It is clearly evident that the excited jet features a shorter potential core and an increased spreading of the shear layer. Note that both figures represent the average flow field using 200 image pairs taken at  $f_s \approx 15Hz$ .

Generally speaking, the roll-up of a natural shear layer is subject to natural disturbances in the flow and hence neither spatially nor temporally fixed. Acoustic excitation, however, causes the roll-up to be more coherent both in time and space. This becomes evident if one takes advantage of the effect of aliasing. This means that if the sampling frequency at which image pairs are recorded is set so that the excitation frequency is an integer multiple of it, one can spatially fix the dynamics of the shear layer for each image pair taken. This is exemplarily shown in Fig.8 c.). One can then, for instance, not only determine the number of vortices per unit time but also if vortices merge together. In the case of Fig.8 c.) it can be seen that three vortices (three velocity peaks along the centreline) are present at any time which also do not undergo pairing (distance  $\Delta x$  between the peaks is constant) and no coherent motion can be observed downstream of the last vortex. Furthermore, for all cases with excitation no pairing events were observed.

Quantitative data of the jet response to acoustic excitation

This is the author's peer reviewed, accepted manuscript. However, the online version of record will be different from this version once it has been copyedited and typeset.

PLEASE CITE THIS ARTICLE AS DOI:10.1063/5.0007934

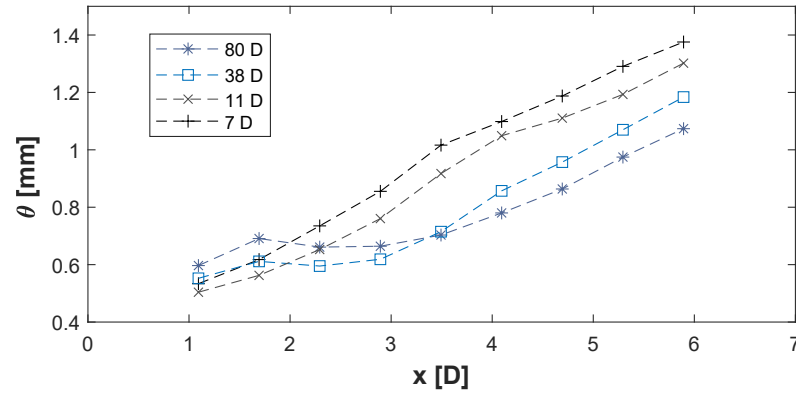


FIG. 6: Boundary layer momentum thickness at different downstream locations for different nozzle lengths  $l_N$

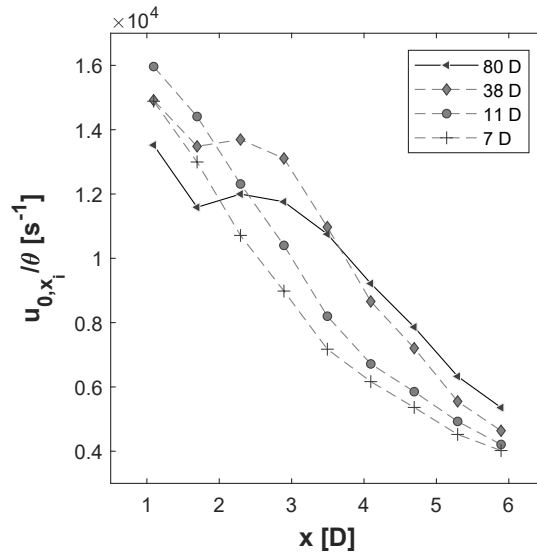


FIG. 7:  $\frac{u_{0,x_i}}{\theta}$  as a measure for the vortex passage frequency along  $x$  assuming a constant non-dimensional frequency  $St_\theta$  for different nozzle lengths  $l_N$

with a forcing level of 2% is displayed in Fig.9 for  $l_N = 80D$ . The jet responds to nearly all excitation frequencies with enhanced mixing. This can be seen by a faster decay of the centreline velocity  $u_0$  and an increase in the momentum thickness  $\theta$ . At  $St_D = 0.3$  the centreline velocity starts to decay almost immediately downstream of the nozzle orifice. The shear layer increase is marginal upstream of  $\frac{x}{D} = 2.5$  but becomes more apparent downstream of that. At  $\frac{x}{D} = 6$  and  $St_D = 0.3$  the shear layer momentum thickness has grown by approximately 60% compared to the baseline case. In order to plot the jet response as function of  $St_D$  based on the spreading of the shear layer, Fig.10 shows the difference in  $\theta$  between each excited case and the baseline case. The values for  $\Delta\theta$  are given in absolute numbers and correspond to the entire momentum thickness integrated from  $-\infty$  to  $\infty$ . Each line in Fig.10 represents a different streamwise location

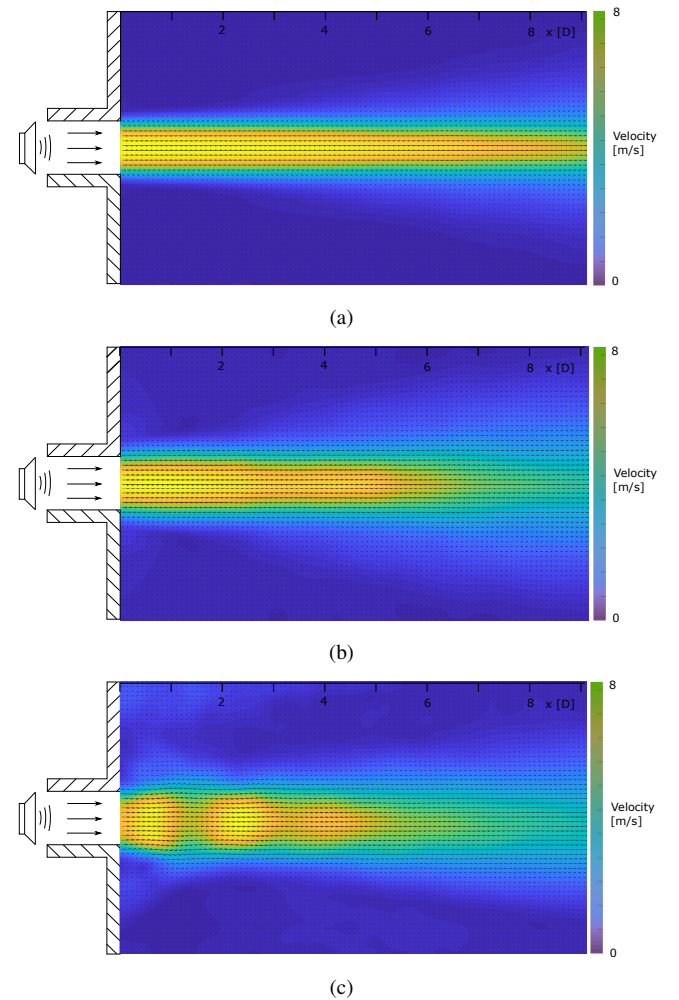


FIG. 8: Mean velocity vector field for  $l_N = 80D$  and  $u_0 = 8 \frac{m}{s}$  using 200 image pairs. a.) Baseline, b.)  $St_D = 0.3$  and  $\frac{u'_0}{u_0} = 2\%$ , c.) Mean velocity field with  $\frac{u'_0}{u_0} = 2\%$  and  $St_D = 0.5$  (aliased sampling frequency)

$x$ . It is obvious that the spreading of the shear layer is highest

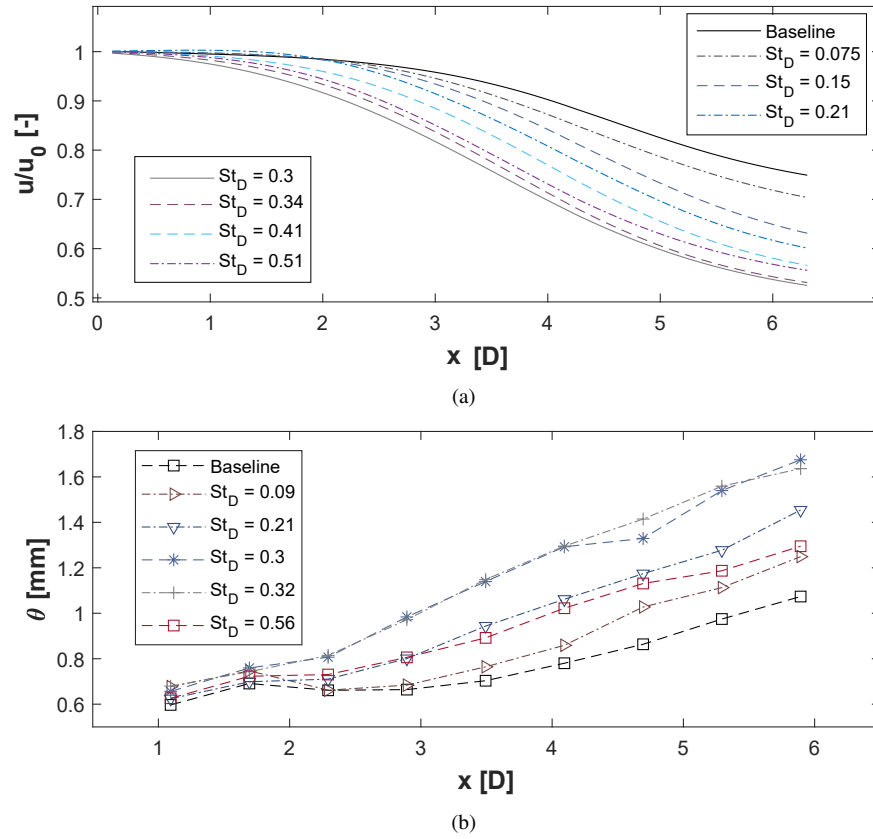


FIG. 9: Flow response to acoustic excitation along  $x$  for  $l_N = 80D$ . a.) Centreline velocity decay, b.) Spreading of the shear layer

around an excitation frequency of  $St_D = 0.3$ . Hence, this can be considered the preferred mode of the jet.

The same conclusion can be drawn from Fig.11 a.) which shows the end of the potential core  $x_{pc}$  as a function of  $St_D$ . It is again obvious that the jet exhibits a maximum response at  $St_D = 0.3$ . Note that  $x_{pc}$  is here arbitrarily defined as the point where 90% of the initial centreline velocity  $u_0$  is reached. Fig.11 b.) further shows the average difference in  $\theta$  along  $x$ , i.e. the mean of Fig.10. It is clearly evident that both graphs serve as a good means to identify the jet preferred mode.

In order to examine the effect of initial conditions on the preferred mode Strouhal number the same set of experiments is repeated for each nozzle length  $l_N$ . Hence, the decay of the centreline velocity as well as the radial velocity profile at  $x_{1-9}$  is determined for each excitation frequency and different  $l_N$ . Unfortunately, no useful data was obtained for  $l_N = 7D$ . The results for the remaining three nozzle lengths are summarized in Fig.12. The jet response for  $l_N = 11D$  shows a strong preference at  $St_D = 0.3$ . Furthermore, the preference is stronger and much more pronounced compared to  $l_N = 80D$ . The length of the jet potential core decreases from  $x_{pc} = 3.5D$  at  $St_D = 0.1$  to  $x_{pc} = 1.5D$  at  $St_D = 0.3$ . There is no apparent effect of excitation around  $St_D = 0.1$  and  $0.6$ . The preference at  $St_D = 0.3$  for  $l_N = 11D$  is less obvious when the increase in  $\theta$  along  $x$  is considered. The maximum spreading of the shear layer is seen to be around  $St_D = 0.3$  but features a rather flat

plateau up to  $St_D = 0.5$ . The overall difference to the baseline case is smaller compared to  $l_N = 80D$ . This is because the baseline case for the shorter nozzle already features a significant larger shear layer as it was seen in Fig.6. Apart from that, the response is seen to be almost the same between  $St_D = 0.25$  and  $0.35$  which shows that the jet preferred mode can only be identified properly if a broad range of excitation frequencies is used. This is rarely the case for other studies done in the past. No distinction in the jet response could be made if the jet was only excited at frequencies between  $St_D = 0.25$  and  $St_D = 0.35$ . This is even more pronounced when looked at the spreading of the shear layer displayed in Fig.12 b.).

The jet response to excitation at  $l_N = 38D$  exhibits a slight difference compared to  $l_N = 80D$  and  $11D$ . The maximum response is obtained at  $St_D = 0.4$  although no real preference can here be deduced since the variation in  $x_{pc}$  between  $St_D = 0.2$  and  $0.5$  amounts to a mere  $0.2D$ . The absolute values for the decrease in  $x_{pc}$  and increase in  $\theta$  are comparable to those at  $l_N = 80D$ .

## V. CONCLUSION

The foundation of the hypothesis made in this paper is based on a constant preferred mode Strouhal number - mea-

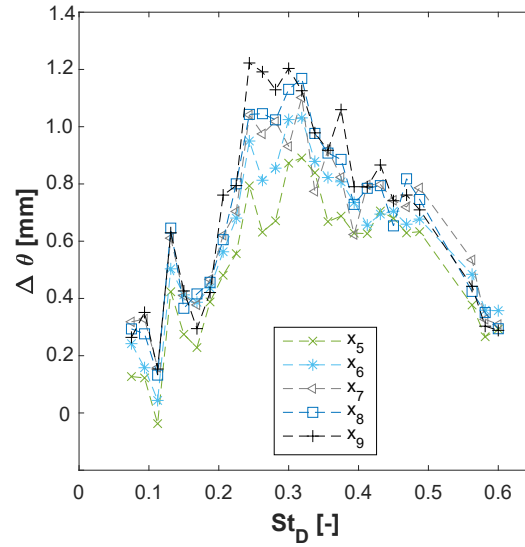
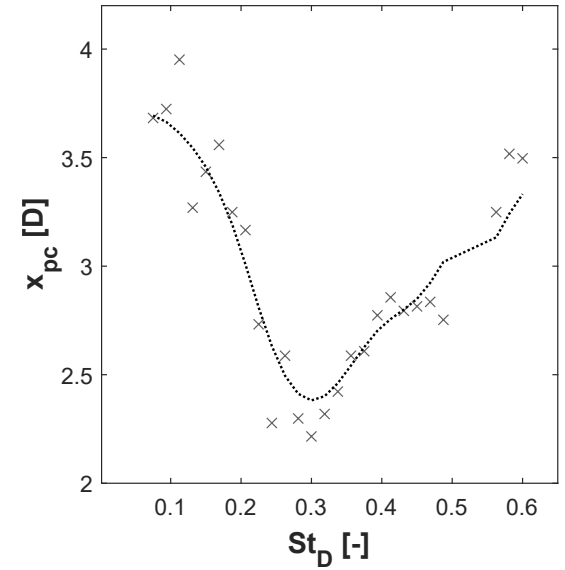


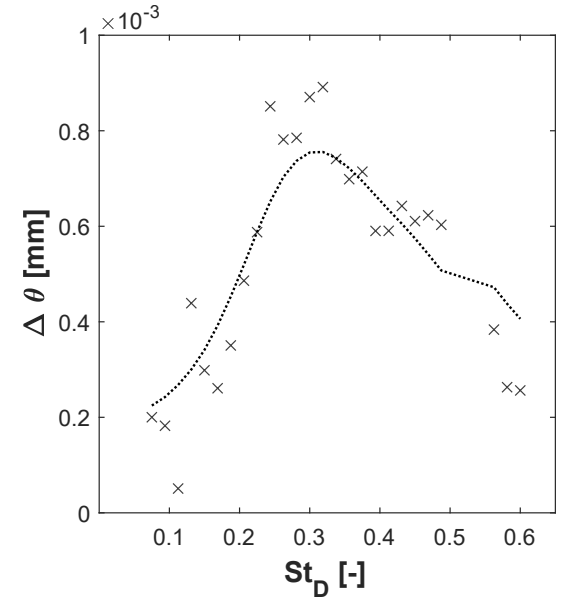
FIG. 10: Increase in  $\theta$  for  $l_N = 80D$  with respect to the baseline case as a function of Strouhal number. Different lines correspond to different downstream locations  $x/D = [5, 6, 7, 8, 9]$

sured via the jet response to acoustic excitation - despite changes in the initial conditions. Considering the results presented above the authors hesitate to draw a decisive conclusion that neither supports nor disputes that hypothesis. On the one hand, the jet preferred mode does indeed seem to remain constant at  $St_D = 0.3$  for  $l_N = 80D$  and  $11D$ . But on the other hand, this would entail that the jet preferred mode is also constant for all nozzle lengths in between. The present results, however, do not allow to conclude that due to the discrepancy of the preferred mode Strouhal number for  $l_N = 38D$ . True, the discrepancy is not huge given that the jet response is rather flat for  $St_D = 0.2 - 0.5$  and one might hesitate to conclude any local preferred mode at all. The uncertainty of the results as well as the already rather small difference in the vortex passage frequency at the end of the potential core between  $l_N = 80D$  and  $11D$ , however, are further reason to skip any unambiguous conclusion.

The question whether the jet preferred mode is independent of the shear layer mode or not still remains unanswered. Fig.1 which showed that the reported value of the jet preferred mode varies considerably less when actual forcing is applied has first been a striking argument in favour of the new hypothesis. However, the huge scatter of the preferred mode Strouhal number for studies without any means of forcing could also be based on the location at which the vortex passage frequency is determined<sup>3</sup>. The convection speed clearly decreases at further downstream positions and so would the frequency of fluctuating entities such as streamwise velocity. This, and of course the change in the passage frequency due to different initial conditions, complicates the identification of a potential jet preferred mode. This means that in case the jet preferred mode relates to the shear layer mode, i.e. by pairing of neighbouring vortices, one would probably expect less



(a) Jet potential core length  $x_{pc}$



(b) Average increase in  $\theta$

FIG. 11: Jet response to acoustic excitation as a function of excitation frequency for  $l_N = 80D$ , a.) Jet potential core length  $x_{pc}$ , b.) Average increase in  $\theta$

scattered data if the response of a jet to excitation is measured rather than the passage frequency at the end of the potential core of an unforced jet. Nevertheless, the authors hope to encourage potential follow-up studies that might come to a more conclusive result.

This is the author's peer reviewed, accepted manuscript. However, the online version of record will be different from this version once it has been copyedited and typeset.

PLEASE CITE THIS ARTICLE AS DOI:10.1063/1.50007934

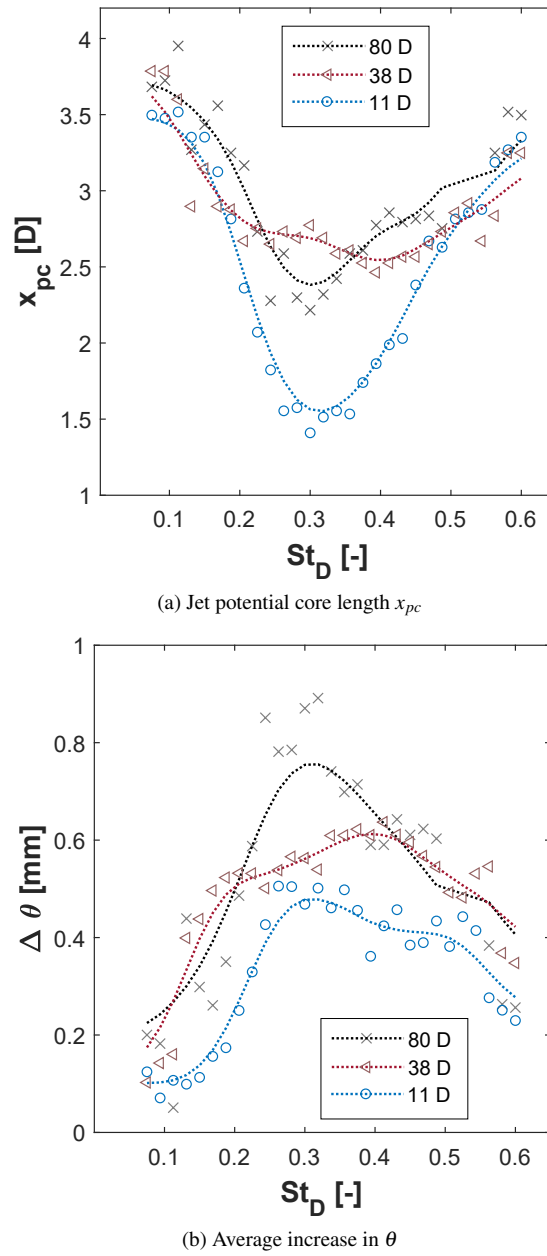


FIG. 12: Jet response to acoustic excitation as a function of excitation frequency and different initial conditions, a.) Jet potential core length  $x_{pc}$ , b.) Average increase in  $\theta$

# ACKNOWLEDGMENTS

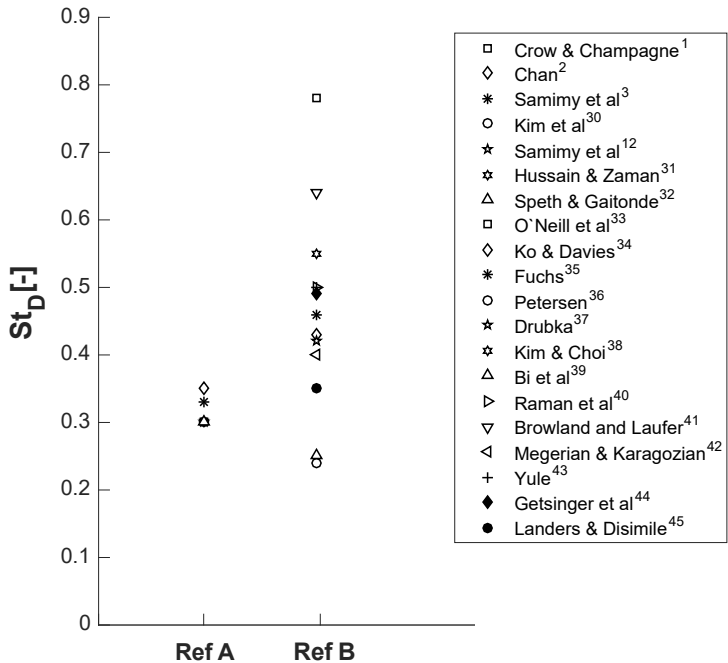
The first two authors wish to acknowledge the support of Ben Williams and Kharthik Chakravarthy regarding the experimental facility. The authors would also like to thank Rolls-Royce plc and the Engineering Physical Sciences Research Council (EP/L015196/1) for funding this work.

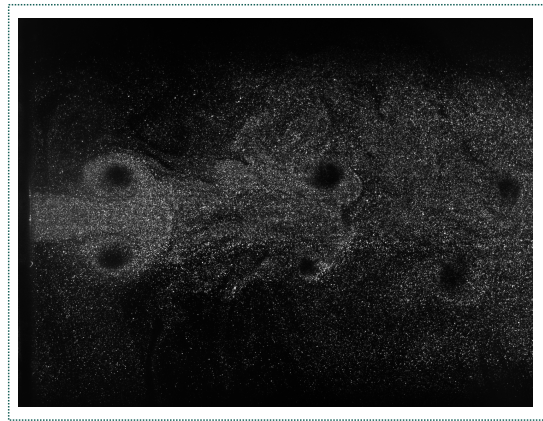
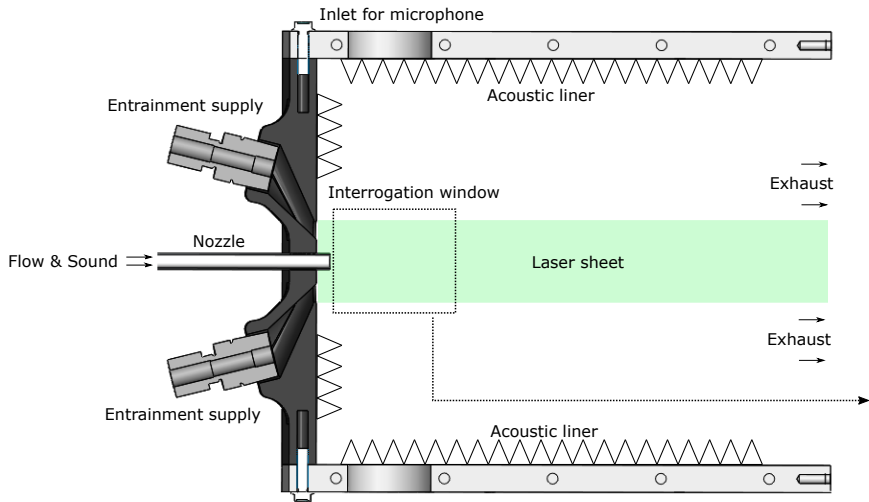
# DATA AVAILABILITY

The data that support the findings of this study are available from the corresponding author upon reasonable request.

- <sup>1</sup>S. C. Crow and F. Champagne, "Orderly structure in jet turbulence," *Journal of Fluid Mechanics* **48**, 547–591 (1971).
- <sup>2</sup>M. Samimy, N. Webb, and M. Crawley, "Excitation of free shear-layer instabilities for high-speed flow control," *AIAA Journal* **56**, 1770–1791 (2018).
- <sup>3</sup>M. Samimy, J.-H. Kim, J. Kastner, I. Adamovich, and Y. Utkin, "Active control of high-speed and high-reynolds-number jets using plasma actuators," *Journal of Fluid Mechanics* **578**, 305–330 (2007).
- <sup>4</sup>E. Gutmark and C.-M. Ho, "Preferred modes and the spreading rates of jets," *The Physics of fluids* **26**, 2932–2938 (1983).
- <sup>5</sup>P. Huerre and P. A. Monkewitz, "Local and global instabilities in spatially developing flows," *Annual review of fluid mechanics* **22**, 473–537 (1990).
- <sup>6</sup>A.-L. Birbaud, D. Durox, S. Ducruix, and S. Candel, "Dynamics of free jets submitted to upstream acoustic modulations," *Physics of Fluids* **19**, 013602 (2007).
- <sup>7</sup>M. Sieber, C. O. Paschereit, and K. Oberleithner, "Spectral proper orthogonal decomposition," *Journal of Fluid Mechanics* **792**, 798–828 (2016).
- <sup>8</sup>O. T. Schmidt and T. Colonius, "Guide to spectral proper orthogonal decomposition," *AIAA Journal* **58**, 1023–1033 (2020).
- <sup>9</sup>O. T. Schmidt, A. Towne, G. Rigas, T. Colonius, and G. A. Brès, "Spectral analysis of jet turbulence," *Journal of Fluid Mechanics* **855**, 953–982 (2018).
- <sup>10</sup>A. Towne, O. T. Schmidt, and T. Colonius, "Spectral proper orthogonal decomposition and its relationship to dynamic mode decomposition and resolvent analysis," *Journal of Fluid Mechanics* **847**, 821–867 (2018).
- <sup>11</sup>G. Rigas, O. T. Schmidt, T. Colonius, and G. A. Brès, "One way navier-stokes and resolvent analysis for modeling coherent structures in a supersonic turbulent jet," in *23rd AIAA/CEAS Aeroacoustics Conference* (2017) p. 4046.
- <sup>12</sup>M. Samimy, J.-H. Kim, M. Kearney-Fischer, and A. Sinha, "Acoustic and flow fields of an excited high reynolds number axisymmetric supersonic jet," *Journal of Fluid Mechanics* **656**, 507–529 (2010).
- <sup>13</sup>C.-W. Kuo, J. Cluts, and M. Samimy, "Effects of excitation around jet preferred mode strouhal number in high-speed jets," *Experiments in Fluids* **58**, 35 (2017).
- <sup>14</sup>A. F. Hussain and K. Zaman, "The 'preferred mode' of the axisymmetric jet," *Journal of fluid mechanics* **110**, 39–71 (1981).
- <sup>15</sup>J. Kastner, J.-H. Kim, and M. Samimy, "Correlation of large-scale structure dynamics and far-field radiated noise in a mach 0.9 jet," in *45th AIAA Aerospace Sciences Meeting and Exhibit* (2007) p. 830.
- <sup>16</sup>K. Zaman and A. Hussain, "Vortex pairing in a circular jet under controlled excitation. part 1. general jet response," *Journal of Fluid Mechanics* **101**, 449–491 (1980).
- <sup>17</sup>R. Betchov and A. Szewczyk, "Stability of a shear layer between parallel streams," *The physics of fluids* **6**, 1391–1396 (1963).
- <sup>18</sup>C. D. Winant and F. K. Browand, "Vortex pairing: the mechanism of turbulent mixing-layer growth at moderate reynolds number," *Journal of Fluid Mechanics* **63**, 237–255 (1974).
- <sup>19</sup>G. L. Brown and A. Roshko, "On density effects and large structure in turbulent mixing layers," *Journal of Fluid Mechanics* **64**, 775–816 (1974).
- <sup>20</sup>Z. Husain and A. Hussain, "Axisymmetric mixing layer: influence of the initial and boundary conditions," *AIAA Journal* **17**, 48–55 (1979).
- <sup>21</sup>C.-M. Ho and L.-S. Huang, "Subharmonics and vortex merging in mixing layers," *Journal of Fluid Mechanics* **119**, 443–473 (1982).
- <sup>22</sup>L. C. Cheung and S. K. Lele, "Linear and nonlinear processes in two-dimensional mixing layer dynamics and sound radiation," *Journal of Fluid Mechanics* **625**, 321–351 (2009).
- <sup>23</sup>R. W. Miksad, "Experiments on the nonlinear stages of free-shear-layer transition," *Journal of Fluid Mechanics* **56**, 695–719 (1972).
- <sup>24</sup>R. Petersen and M. Samet, "On the preferred mode of jet instability," *Journal of Fluid Mechanics* **194**, 153–173 (1988).
- <sup>25</sup>V. Kibens, "Discrete noise spectrum generated by acoustically excited jet," *AIAA Journal* **18**, 434–441 (1980).

- <sup>26</sup>D. Bechert and E. Pfizenmaier, "On the amplification of broad band jet noise by a pure tone excitation," *Journal of Sound and Vibration* **43**, 581–587 (1975).
- <sup>27</sup>A. Cavalieri, P. Jordan, Y. Gervais, M. Wei, and J. Freund, "Intermittent sound generation in a free-shear flow," in *16th AIAA/CEAS Aeroacoustics Conference* (2010) p. 3963.
- <sup>28</sup>J. Bridges and A. Hussain, "Roles of initial condition and vortex pairing in jet noise," *Journal of Sound and Vibration* **117**, 289–311 (1987).
- <sup>29</sup>Y.-Y. Chan, "Spatial waves in turbulent jets," *The Physics of Fluids* **17**, 46–53 (1974).
- <sup>30</sup>J.-H. Kim, J. Kastner, and M. Samimy, "Active control of a high reynolds number mach 0.9 axisymmetric jet," *AIAA Journal* **47**, 116–128 (2009).
- <sup>31</sup>A. Hussain and K. Zaman, "Controlled perturbation of circular jets," in *Structure and Mechanisms of Turbulence I* (Springer, 1978) pp. 31–42.
- <sup>32</sup>R. Speth and D. V. Gaitonde, "Parametric study of a mach 1.3 cold jet excited by the flapping mode using plasma actuators," *Computers & Fluids* **84**, 16–34 (2013).
- <sup>33</sup>P. O'Neill, J. Soria, and D. Honnery, "The stability of low reynolds number round jets," *Experiments in fluids* **36**, 473–483 (2004).
- <sup>34</sup>N. Ko and P. Davies, "The near field within the potential cone of subsonic cold jets," *Journal of Fluid Mechanics* **50**, 49–78 (1971).
- <sup>35</sup>H. V. Fuchs, "Measurement of pressure fluctuations within subsonic turbulent jets," *Journal of Sound and Vibration* **22**, 361–378 (1972).
- <sup>36</sup>R. Petersen, "Influence of wave dispersion on vortex pairing in a jet," *Journal of Fluid Mechanics* **89**, 469–495 (1978).
- <sup>37</sup>R. E. Drubka, *Instabilities in near field of turbulent jets and their dependence on initial conditions and Reynolds number.*, Ph.D. thesis, Illinois Institute of Technology, Chicago (1981).
- <sup>38</sup>J. Kim and H. Choi, "Large eddy simulation of a circular jet: effect of inflow conditions on the near field," *Journal of Fluid Mechanics* **620**, 383–411 (2009).
- <sup>39</sup>W. Bi, Y. Sugii, K. Okamoto, and H. Madaram, "Time-resolved proper orthogonal decomposition of the near-field flow of a round jet measured by dynamic particle image velocimetry," *Measurement Science and Technology* **14**, L1 (2003).
- <sup>40</sup>G. Raman, E. Rice, and E. Reshotko, "Mode spectra of natural disturbances in a circular jet and the effect of acoustic forcing," *Experiments in fluids* **17**, 415–426 (1994).
- <sup>41</sup>F. Browand and J. Laufer, "The roles of large scale structures in the initial development of circular jets," (1975).
- <sup>42</sup>S. Megerian and A. Karagozian, "Evolution of shear layer instabilities in the transverse jet," in *43rd AIAA Aerospace Sciences Meeting and Exhibit* (2005) p. 142.
- <sup>43</sup>A. Yule, "Large-scale structure in the mixing layer of a round jet," *Journal of Fluid Mechanics* **89**, 413–432 (1978).
- <sup>44</sup>D. R. Getsinger, C. Hendrickson, and A. R. Karagozian, "Shear layer instabilities in low-density transverse jets," *Experiments in fluids* **53**, 783–801 (2012).
- <sup>45</sup>B. D. Landers and P. J. Disimile, "Passing frequency of vortical structures in the near field of an axisymmetric turbulent jet," *Int J Mech Eng* **2**, 14–18 (2015).
- <sup>46</sup>S. Russ and P. Strykowski, "Turbulent structure and entrainment in heated jets: The effect of initial conditions," *Physics of Fluids A: Fluid Dynamics* **5**, 3216–3225 (1993).
- <sup>47</sup>G. Xu and R. Antonia, "Effect of different initial conditions on a turbulent round free jet," *Experiments in Fluids* **33**, 677–683 (2002).
- <sup>48</sup>A. Hussain and M. Zedan, "Effects of the initial condition on the axisymmetric free shear layer: Effects of the initial momentum thickness," *The Physics of Fluids* **21**, 1100–1112 (1978).
- <sup>49</sup>A. Hussain and M. Zedan, "Effects of the initial condition on the axisymmetric free shear layer: Effect of the initial fluctuation level," *The Physics of Fluids* **21**, 1475–1481 (1978).
- <sup>50</sup>W. K. George, "The self-preservation of turbulent flows and its relation to initial conditions and coherent structures," *Advances in turbulence* **3973** (1989).
- <sup>51</sup>X. Grandchamp and A. Van Hirtum, "Near field round jet flow downstream from an abrupt contraction nozzle with tube extension," *Flow, turbulence and combustion* **90**, 95–119 (2013).
- <sup>52</sup>R. Antonia and Q. Zhao, "Effect of initial conditions on a circular jet," *Experiments in fluids* **31**, 319–323 (2001).



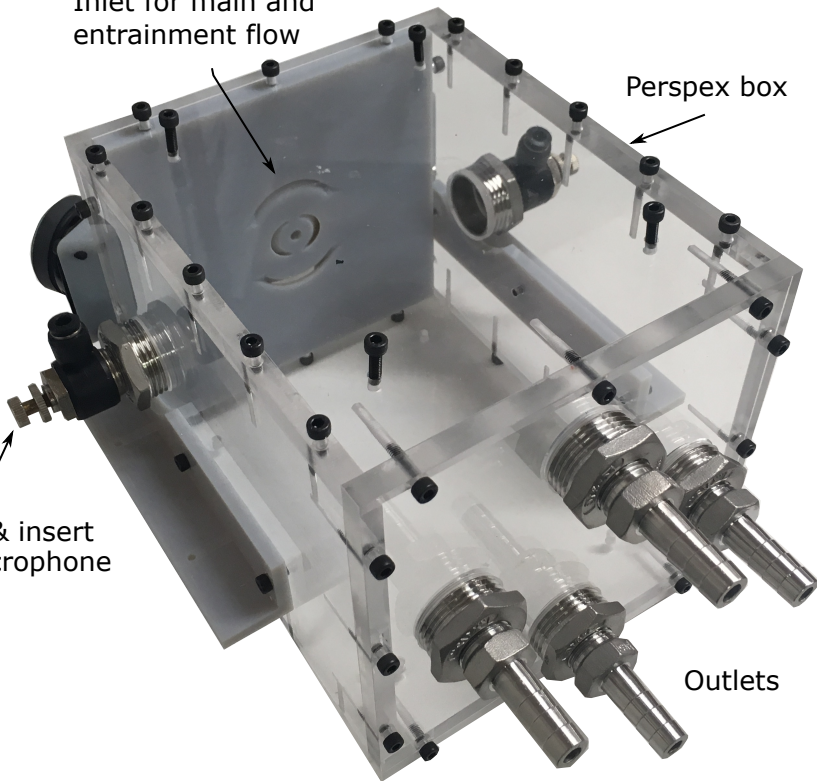


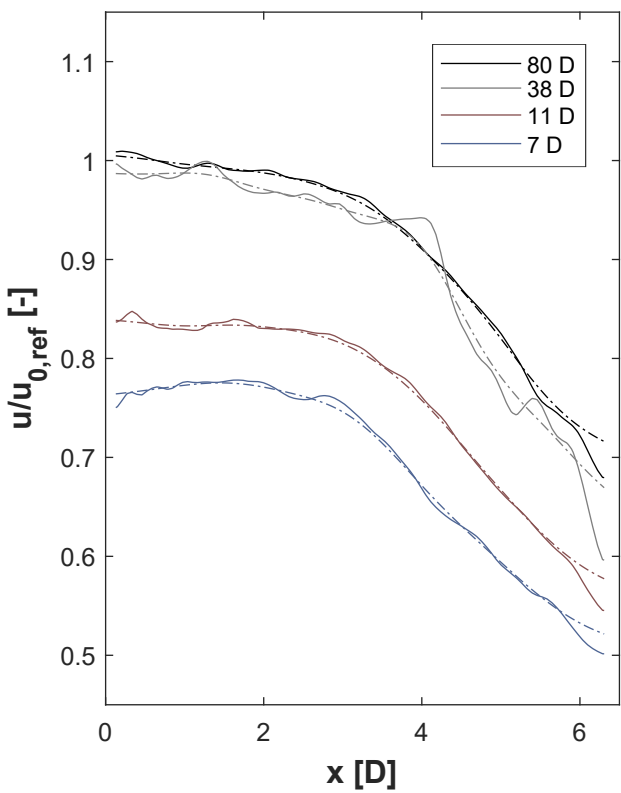
Inlet for main and  
entrainment flow

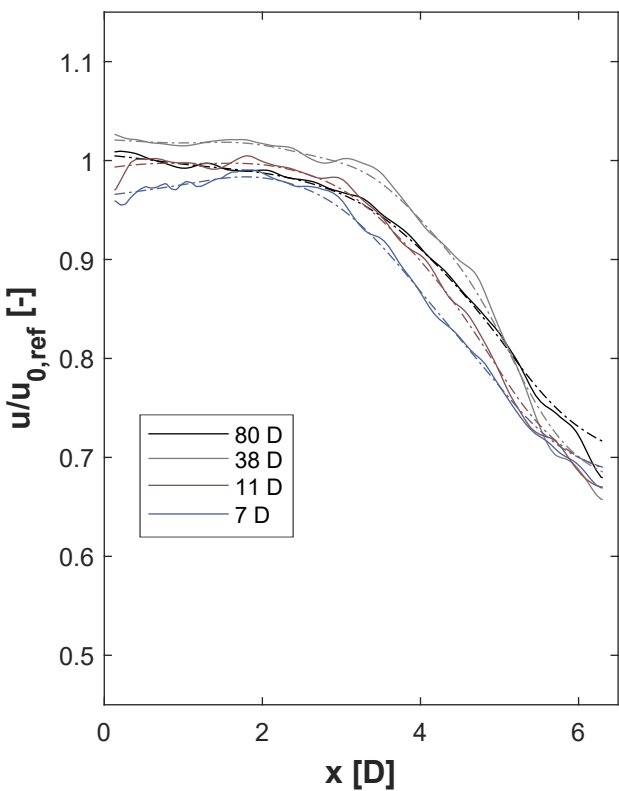
Perspex box

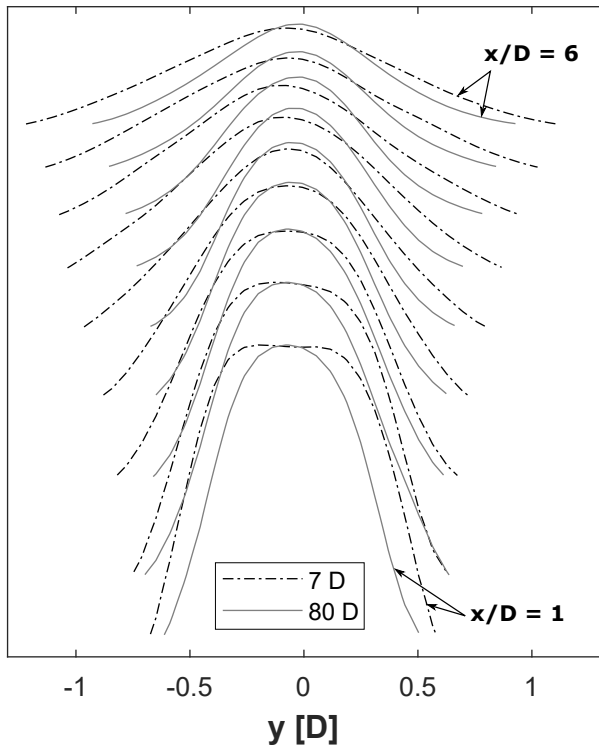
Valve & insert  
for microphone

Outlets

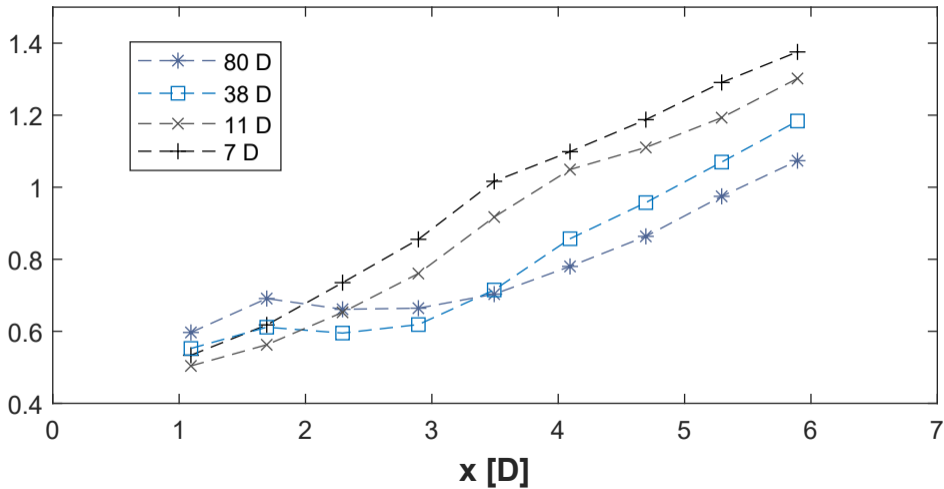


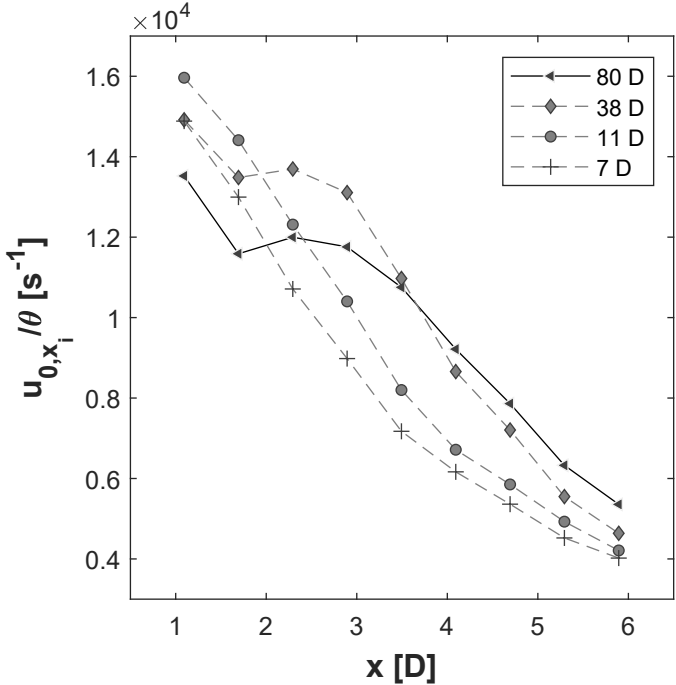


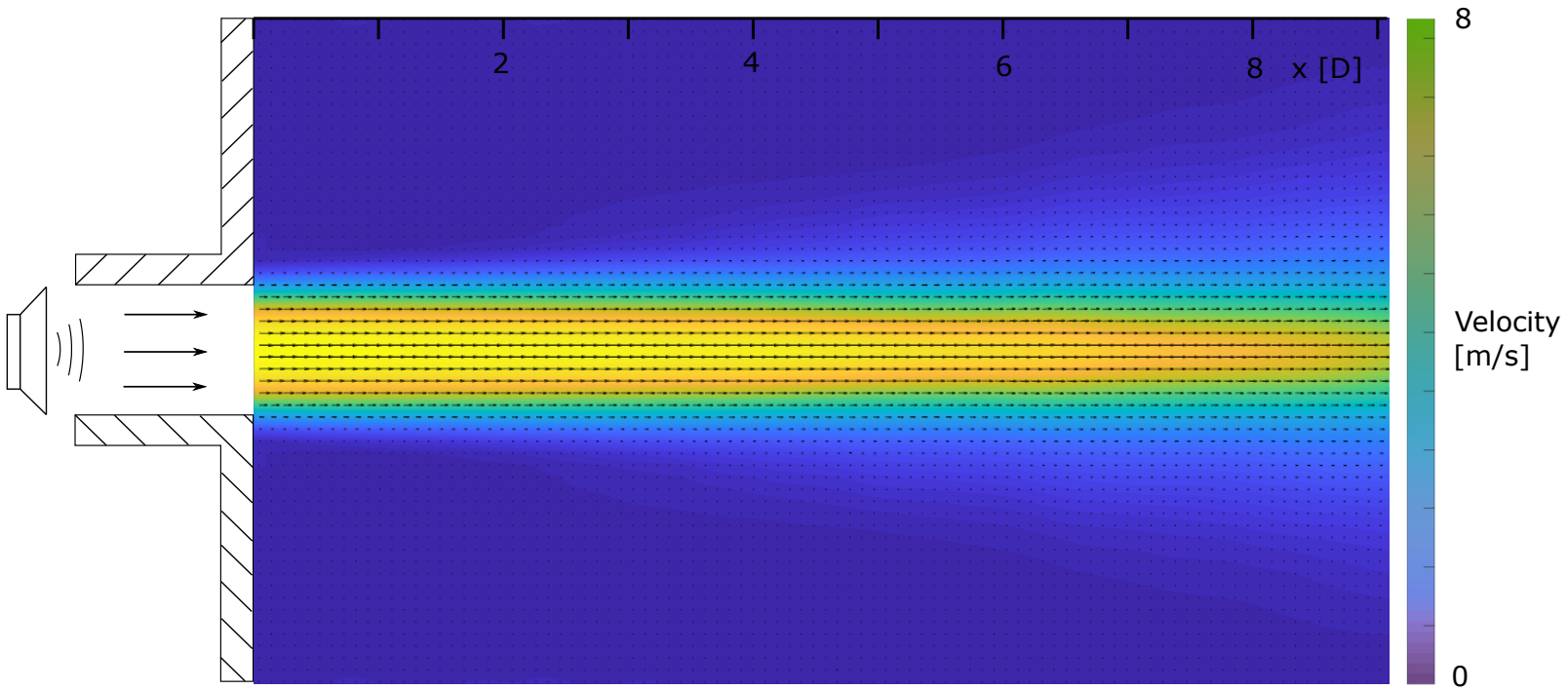


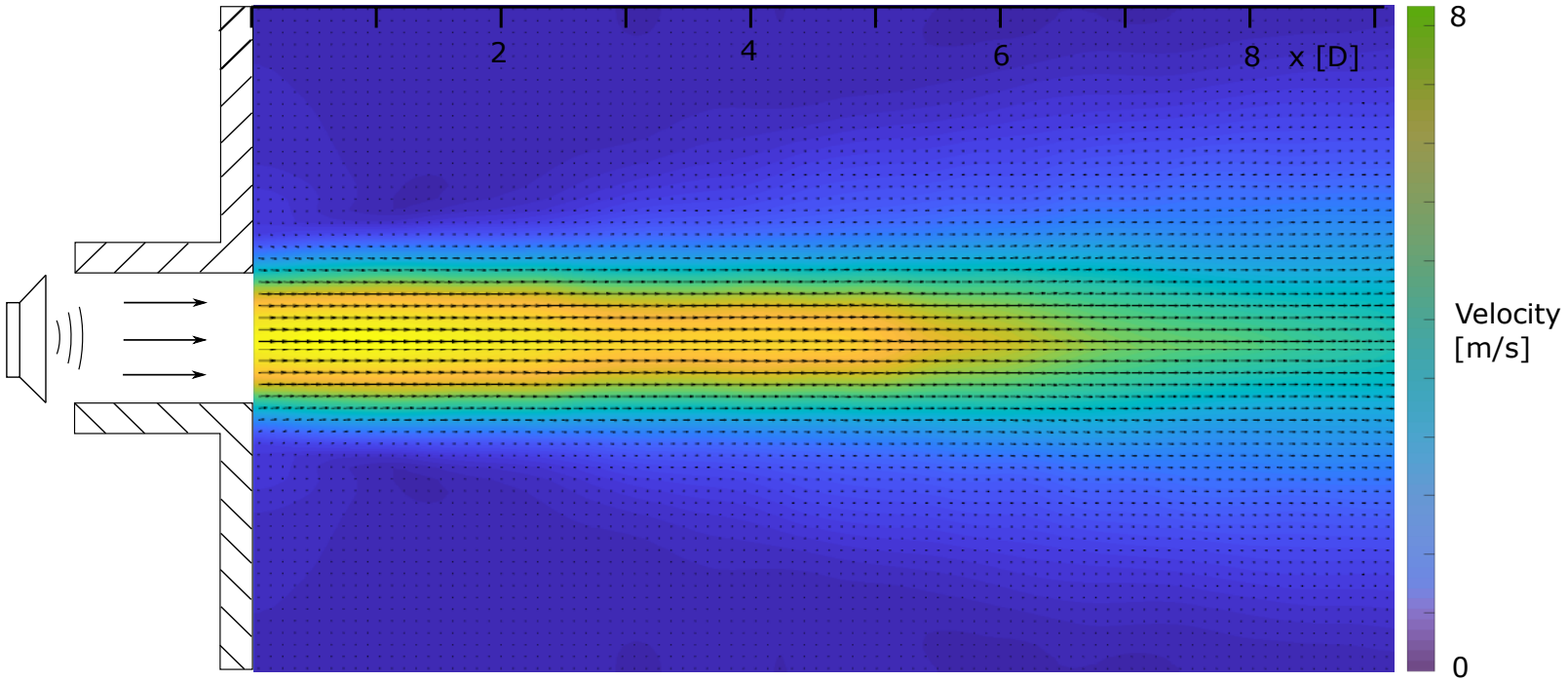


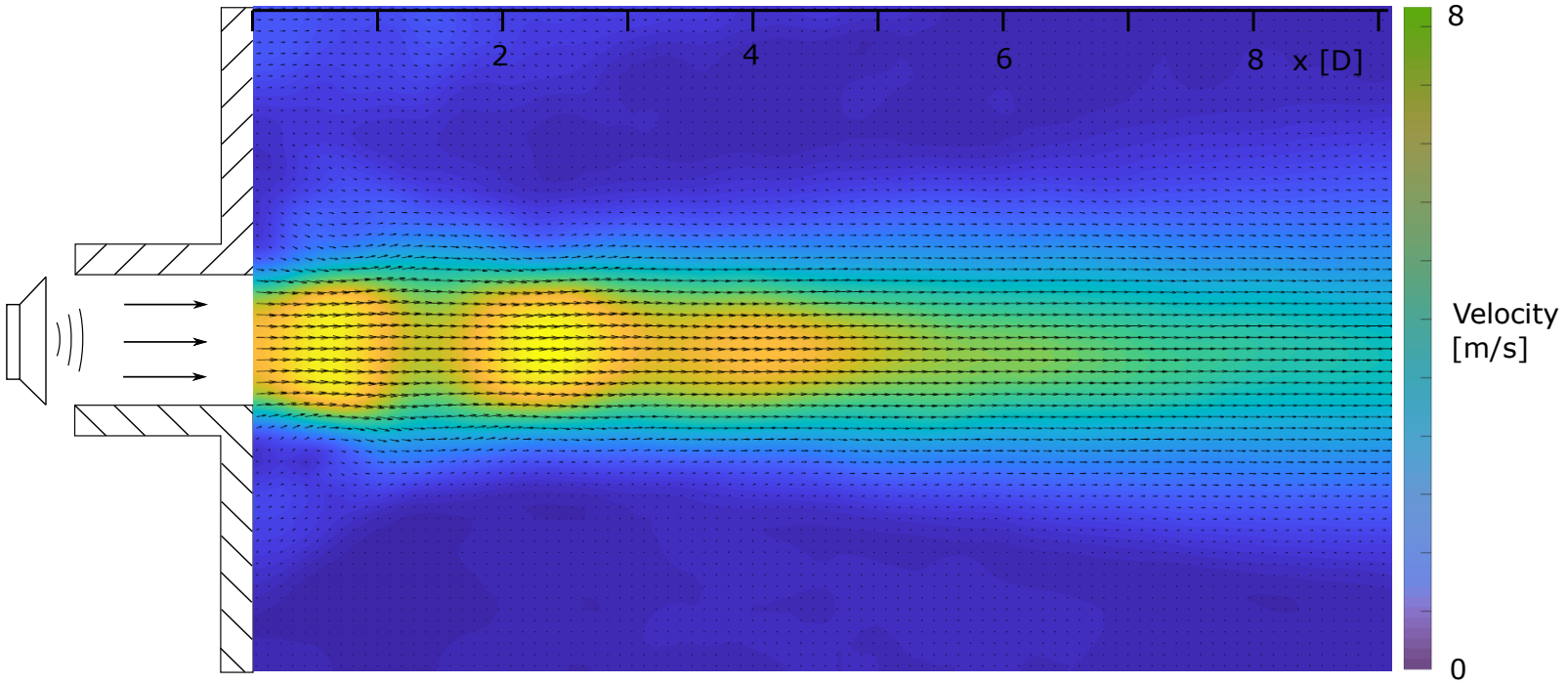
$\theta$  [mm]



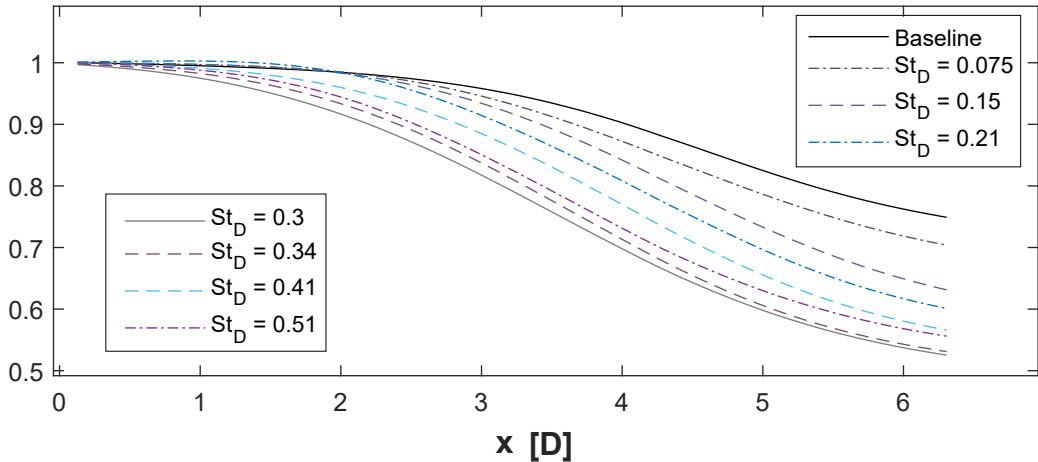


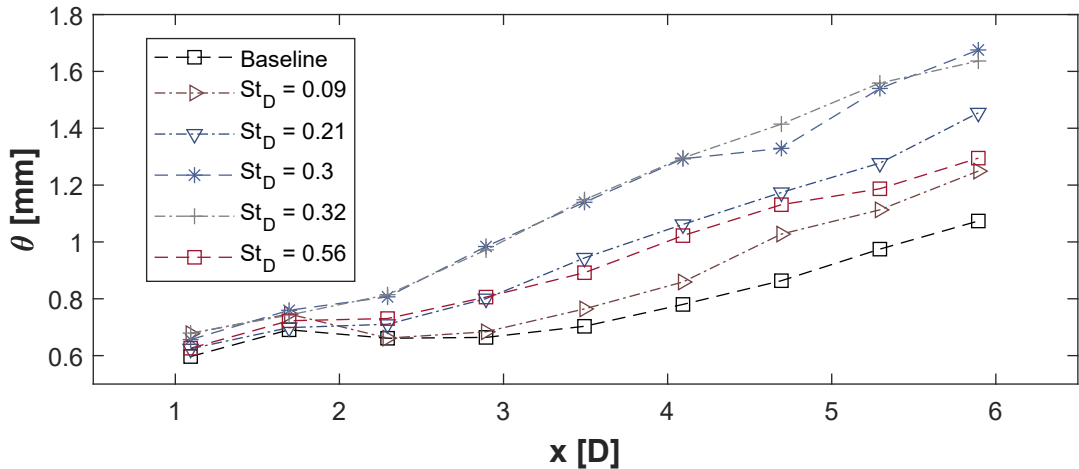


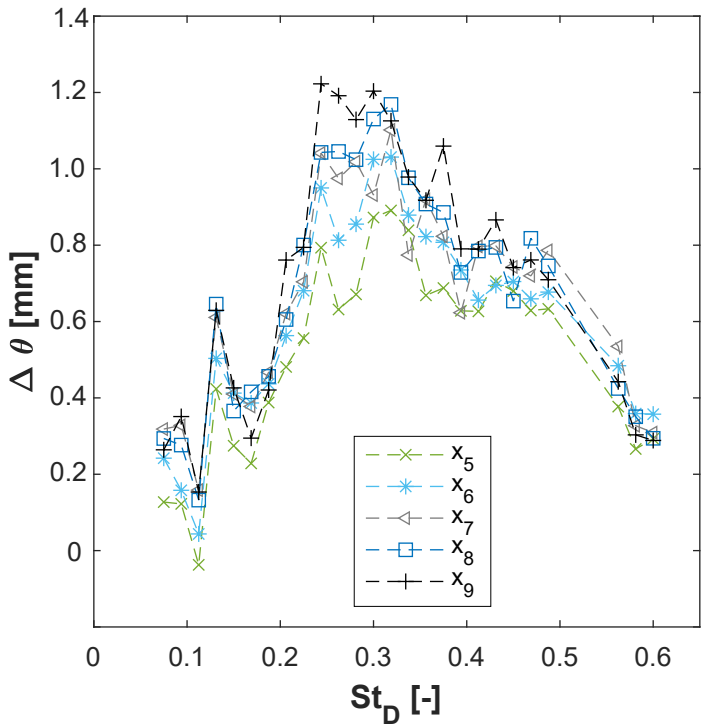


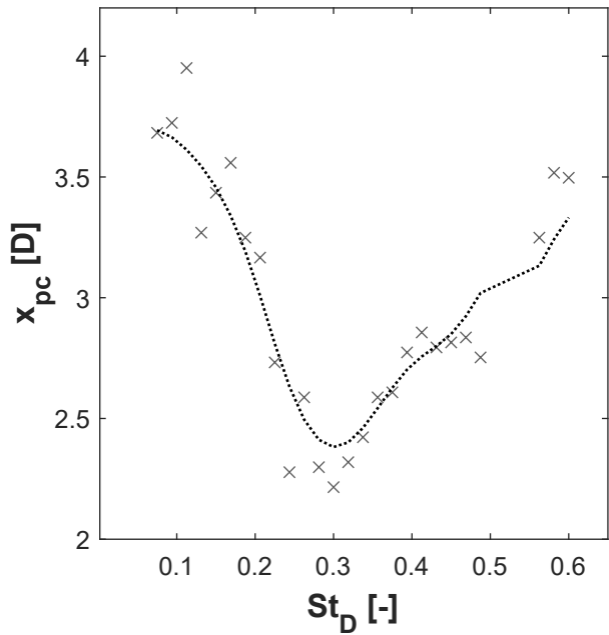


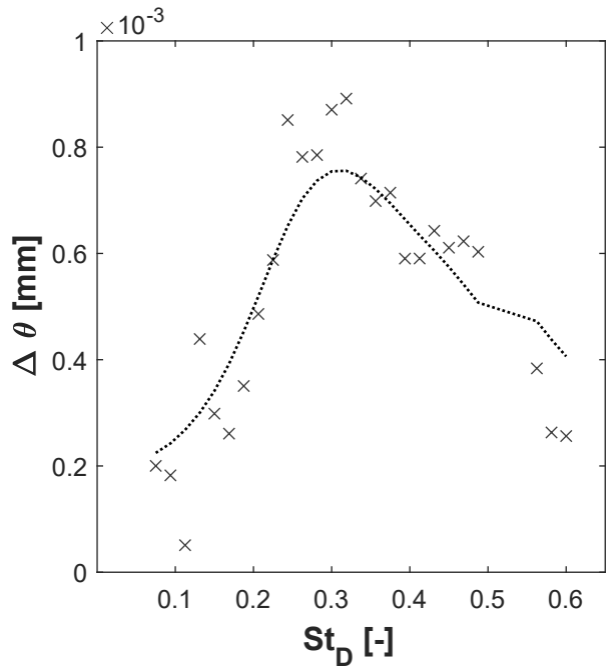
$u/u_0$  [-]











$x_{pc}$  [D]

